Experimental characterization and correction of non-equivalence of Solar Irradiance Absolute Radiometer

Zhenling Yang (杨振岭)*, Wei Fang (方 伟), Yang Luo (骆 杨), and Zhiwei Xia (夏志伟)

Changchun Institute of Optics, Fine Mechanics and Physics, Chinese Academy of Sciences, Changchun 130033, China

**Corresponding author: yangzl@ciomp.ac.cn*

Received March 16, 2014; accepted July 16, 2014; posted online September 3, 2014

We experimentally evaluate and correct the non-equivalence between electrical and radiative heating of solar irradiance absolute radiometer to compensate the systematic error of radiant power measurement at ambient pressure. A relative difference of the order of 0.08%–0.27% between electrical and radiative heating sensitivities is shown, and the resulting non-equivalence correction factor is calculated. The radiant power measurement equation is modified using the non-equivalence correction factor, a systematic deviation of 0.19% of radiant power measurement is hence eliminated.

OCIS codes: 120.3930, 120.3940, 120.5630.
doi: 10.3788/COL201412.101202.

Solar radiation is the most important external energy source for the climate system of the Earth. It drives climate process such as the evaporation of water from the oceans and land and the convection in the atmosphere. It is essential to realize the global energy budget of the Earth[1] to understand the long-term climate changes. The short-term weather changes are also associated with solar radiation through the clouds such as cirrus[2,3]. Abbot *et al.*'s[4] observational results claimed variations of several percent of the total solar irradiance arriving at the top of the atmosphere on short-term periodic timescales. Since late 1970s, the satellite-based measurements of total solar irradiance have been started, which reveals the variation of the total solar irradiance and the correlation with the sunspot number. The amplitude of the variation is 0.1% during an 11-year solar cycle[5]. The driving effect of solar radiation on the Earth's climate system was estimated based on the data measured by spaceborne radiometers during the last three solar cycles[6]. The long-term high-precision measurement of total solar irradiance is required for the climate science and solar physics investigations.

The spaceborne total solar irradiance radiometer is the absolute electrical substitution radiometer. The absolute value of total solar irradiance is measured by determining the solar radiant power received through an aperture with known area. The precision aperture is usually made of weak heat transfer material, such as stainless steel, and the front surface is nickel plated to prevent radiative heating. The aperture area can be determined at high accuracy by using an optical method[7]. Solar radiation is absorbed in a cavity with high absorptivity, resulting in a temperature rise. The temperature rise of cavity is electrically calibrated, hence the solar radiant power can be determined by calculating the equivalent electrical power. The precondition of the measurement procedure is that the electrical and radiative heating sensitivities of the cavity are equivalent, whereas the difference of these two sensitivities is affirmed, which is entitled non-equivalence[8–10]. The non-equivalence is due to the differences in the heating power distribution and thermal diffusion in the cavity during the shaded electrical heating and irradiated radiative heating sequences. According to the measurements using Total Irradiance Monitor (TIM)[11] on Solar Radiation and Climate Experiment and Solar Variability Picard[12], the latest accurate value of total solar irradiance was 1360.8–1362.1 W/m^2, a significant systematic deviation from the canonical value of 1365.4 ± 1.3 W/m^2 established in the 1990s was exhibited. As a main radiation measurement systematic deviation origin, non-equivalence is corrected for different types of radiometers, such as Physikalisch Meteorologisches Observatorium Radiometer[9], TIM[10], and Differential Absolute Radiometer[13]. The systematic error of radiation measurement was compensated by correcting non-equivalence, furthermore the offsets between different total solar irradiance radiometers were shortened, which was advantageous for the continuity of total solar irradiance onboard observation.

Here the framework and measurement procedure of Solar Irradiance Absolute Radiometer (SIAR)[14–16] manufactured in our research group are depicted. The sensitivities of SIAR during the shaded electrical heating and irradiated radiative heating sequences were alternately determined in vacuum and at ambient pressure. The two sensitivities measured at ambient pressure represented a difference of the order of 0.08%–0.27%.

The correction for non-equivalence of SIAR was defined to be the air-to-vacuum ratio of the sensitivity of SIAR as measured with an invariable light source minus the air-to-vacuum ratio measured with electrical heating. With the correction for non-equivalence of SIAR, the radiant power measurement equation at ambient pressure was modified, which compensated the systematic error of radiant power measurement.

SIAR is an electrical substitute radiometer. A schematic drawing of SIAR is shown in Fig. 1. Heat loaded in the main cavity is conducted to the heat sink of the instrument, and the resulting temperature difference across the thermocouples is sensed. In order to shield the cavity temperature changes caused by the heat sink temperature fluctuations, a compensation cavity was adopted, which was made using the same production and assembly processes as the main cavity. The low-level thermocouples of the main cavity were attached to the high-level thermocouples of the compensation cavity, and the low-level thermocouples of the compensation cavity were grounded. Thus the temperature rise measured by the thermocouples of the main cavity is only caused by the heating power loaded in it. The sensitivity of the thermocouples of the main cavity is calibrated by measuring the temperature difference with a known amount of electrical power dissipated in the electrical heater when the main cavity is shaded. After the shutter is opened, the main cavity which ensures a high absorptivity over the spectral range absorbs the radiant power, the thermocouples sense the temperature rise, and the radiant power can be calculated with the calibrated sensitivity and the temperature rise.

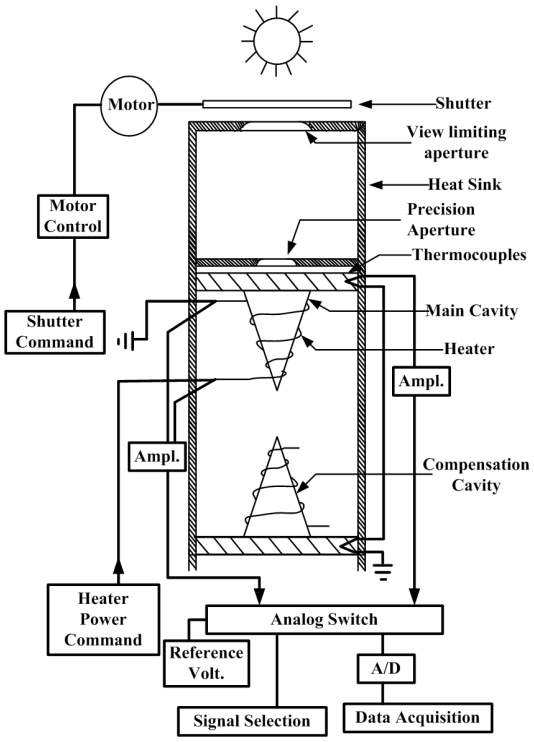

Fig. 1. Schematic representation of SIAR with its control electronics.

The practical operation procedure of SIAR consists of a self-test process and a solar measurement process[14]. During the self-test process, the shutter is closed. A low-electrical power P_{L} and a high-electrical power P_{H} are dissipated successively in the electrical heater, the thermocouples detect the temperature difference in each state and output a voltage after equilibrium (V_{EL} and V_{EH}), respectively. The sensitivity of the thermocouples calibrated by electrical power S_{E} can be described as

$$S_{\mathrm{E}} = \frac{V_{\mathrm{EH}} - V_{\mathrm{EL}}}{P_{\mathrm{H}} - P_{\mathrm{L}}}. \tag{1}$$

In the initial stage of the solar measurement process, a higher electrical power is dissipated in the electrical heater to ensure that the main cavity temperature is maintained at high level. For SIAR this higher electrical power is set to 75 mW. After the shutter is opened, the main cavity absorbs the radiant power P_{R}, the electrical power dissipated in the heater is reduced to be P_1 in order to avoid large fluctuations in cavity temperature[16]. The thermocouples output an equilibrium voltage V_{E1}. Then, the main cavity is shaded, an electrical heating power P_2, which is close to 75 mW, is loaded in the heater, the thermocouples output an equilibrium voltage V_{E2}. The relationship between the heating powers and equilibrium temperatures during the two stages can be depicted as

$$\begin{cases} P_{\mathrm{R}} S_{\mathrm{R}} + P_1 S_{\mathrm{E}} + V_{\mathrm{E}} = V_{\mathrm{E1}} \\ P_2 S_{\mathrm{E}} + V_{\mathrm{B}} = V_{\mathrm{E2}} \end{cases}, \tag{2}$$

where S_{R} is the radiative heating sensitivity of thermocouples and V_{B} is the offset of the thermocouples output. The radiant power absorbed in the main cavity P_{R} can be calculated by

$$P_{\mathrm{R}} = \frac{\left(P_2 - P_1\right) S_{\mathrm{E}} - \left(V_{\mathrm{E2}} - V_{\mathrm{E1}}\right)}{S_{\mathrm{R}}}. \tag{3}$$

When the non-equivalence of the instrument is ignored, that is, $S_{\mathrm{E}} = S_{\mathrm{R}}$, P_{R} should be

$$P_{\mathrm{R}} = P_2 - P_1 - \frac{V_{\mathrm{E2}} - V_{\mathrm{E1}}}{S_{\mathrm{E}}}. \tag{4}$$

The correction factor for non-equivalence of SIAR at ambient pressure is defined by[9]

$$k = \frac{S_{\mathrm{AR}}}{S_{\mathrm{VR}}} - \frac{S_{\mathrm{AE}}}{S_{\mathrm{VE}}}, \tag{5}$$

where S_{VR} and S_{AR} are radiative heating sensitivities in vacuum and at ambient pressure, respectively, and S_{VE} and S_{AE} are electrical heating sensitivities in vacuum and at ambient pressure, respectively. In view of the structure and blackening technology of the cavity and the location of the heater[14], it is reasonable to assume

that the non-equivalence can be neglected when air convection is removed in vacuum, thus $S_{VE} = S_{VR}$.

In order to determine these sensitivities, SIAR was placed in a vacuum chamber with a quartz window. A bromine tungsten lamp (24 V and 150 W) was used as a light source, which was lightened by a regulated power supply (N5770A, Agilent). The stability of radiant power absorbed in the main cavity was ensured since the regulated power supply and immobile light path setup. Table 1 lists the continuous measurement results of the light source power absorbed in the main cavity of SIAR at an immobile setup. The repeatability was calculated to be 0.026%. The light irradiated SIAR through the quartz window. After the light source warmed up, standard measurement procedure of SIAR was repeatedly run in vacuum, which included the self-test and solar measurement processes. The sensitivity S_{VE} and radiant power absorbed in the cavity P_R were calculated according to Eqs. (1) and (4).

The pressure in the vacuum chamber was then restored to ambient pressure. The radiant power absorbed in the main cavity was corrected to P_R with the atmospheric absorption between quartz window and SIAR in the chamber. Lower solution transmission program was adopted to calculate the atmospheric transmittance, in which the US Standard Atmospheric model was used. The atmospheric depth was set to be 1 m, which was the distance between the precision aperture of SIAR and the entrance window of the vacuum chamber. The emission spectrum of the lamp is equivalent to that of a 2900 K blackbody, which can be depicted by Planck's blackbody radiation law. The atmospheric absorption coefficient was calculated to be 2.8% with the emission of the lamp and the atmospheric transmittance spectral curves. The standard measurement procedure of SIAR was run repeatedly at ambient pressure. The sensitivity S_{AE} was calculated using Eq. (1), and the sensitivity S_{AR} was calculated with the corrected P_R^* using Eq. (3). The correction factor for non-equivalence of SIAR at ambient pressure was determined based on these sensitivities and Eq. (4). The radiant power measurement equation was modified at last.

Table 1. Light Source Stability Measurement Results

	Measured Radiative Power Absorbed by SIAR (mW)
1	68.852
2	68.905
3	68.904
4	68.902
5	68.895
6	68.870
7	68.888
8	68.902
9	68.867
10	68.888
Average Value	68.888
Standard Deviation	0.018
Relative Error	0.026%

The heating-up processes of the main cavity in vacuum and at ambient pressure were investigated firstly, while the same electrical heating power dissipated in the heater. Figure 2 shows the heating-up processes and their fitting curves. The heating-up process of the main cavity follows single exponential function[16]. The fitting results indicate that heating-up process is slower in vacuum because the air convection is removed. The time constant changed from 12.86 s at ambient pressure to 25.44 s in vacuum. It is reasonable to set the sampling time to be 300 s since an equilibrium voltage of the thermocouples output could be achieved both in vacuum and at ambient pressure, as shown in Fig. 2. The equilibrium voltages in these two working environments are obviously different, which implies the difference in the sensitivities to electrical heating power in vacuum and at ambient pressure.

In order to quantitatively research the difference in the electrical heating sensitivities of the thermocouples in the two working environments, three electrical heating powers (10, 45, and 75 mW) were dissipated in the heater successively, and the respective equilibrium voltage of the thermocouples were recorded. Figure 3 shows the dissipated electrical powers and corresponding equilibrium voltages. The electrical heating sensitivities and offset of thermocouples in these two working environments were determined by linear fitting. Compared with the electrical heating sensitivity at ambient pressure $S_{AE} = 58.833$ V/W, the electrical heating sensitivity in vacuum was increased about 19.3%, to be $S_{VE} = 70.201$ V/W.

The radiant power absorbed in the main cavity was detected repeatedly by running the standard measurement

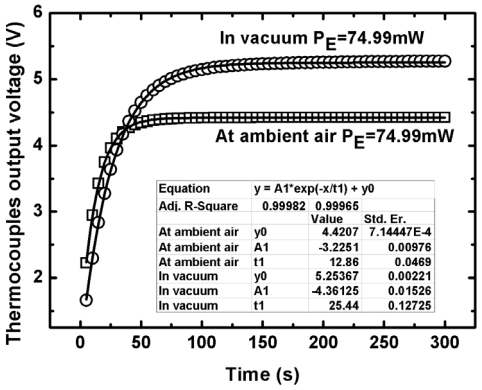

Fig. 2. Heating-up curves of the main cavity in vacuum (○) and at ambient pressure (□).

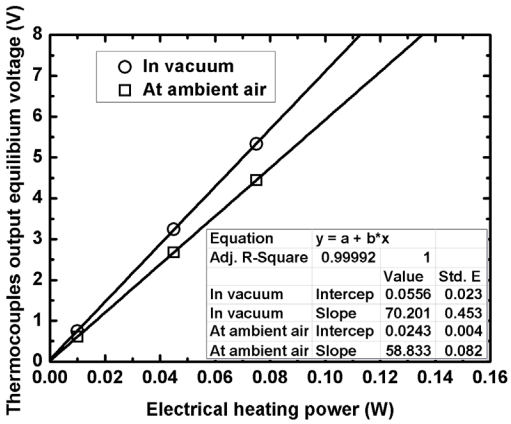

Fig. 3. Electrical heating power dissipated in the heater and the thermocouples output equilibrium voltages of a correspondence.

Table 3. Correction for Non-equivalence Measurement Results at Ambient Pressure

	(1)	(2)	(3)
S_{AE}(V/W)	58.833	58.767	58.788
P_1 (mW)	39.463	39.530	39.407
P_2 (mW)	76.507	76.328	76.162
V_{E1} (V)	4.503	4.487	4.477
V_{E2} (V)	4.585	4.558	4.545
S_{AR} (V/W)	58.784	58.609	58.667
k	–0.0007	–0.0023	–0.0017

procedure of SIAR in vacuum. Table 2 shows the calculated results. The absorbed radiant power in the main cavity at ambient pressure was determined to be 35.684 mW based on the average value detected in vacuum and the atmospheric absorption coefficient. The standard measurement procedure of SIAR was run at ambient pressure, resulting data are given in Table 3. According to the known absorbed radiant power, the radiative heating sensitivity S_{AR} was calculated according to Eq. (3). Compared with the electrical heating sensitivity S_{AE}, S_{AR} reveals a decrease in the order of 0.08%–0.27%. The correction factor for non-equivalence of SIAR at ambient pressure was obtained according to Eq. (5).

The non-equivalence of SIAR working at ambient pressure was affirmed and characterized experimentally, hence after the standard measurement procedure, the calculation equation of the absorbed radiant power in the main cavity should be modified as

$$P_R = \frac{\left(P_2 - P\right)_1 S_E - \left(V_{E2} - V_{E1}\right)}{S_{AE} + kS_{VE}}. \quad (6)$$

The effect of non-equivalence correction of SIAR was estimated, using an average value of k and S_{VE}, as shown in Fig. 4. Compared with the absorbed radiant power calculated by the measured values in vacuum and atmospheric absorption correction shown by boxes on the right side of Fig. 4, the measured radiant power values without non-equivalence corrected shown by triangles on the left side of Fig. 4 put up a global systematic deviation of the order of 0.19%. The radiant power values with non-equivalence corrected are shown by circles in the middle of Fig. 4. The systematic deviation is eliminated.

In conclusion, we experimentally investigate the responses of thermocouples in SIAR in vacuum and at ambient pressure. When the same electrical heating power is dissipated in the heater, the main cavity shows a slow heating-up rate and a high-electrical heating sensitivity in vacuum compared with those at ambient pressure. By running the standard measurement procedure of SIAR, the radiant power absorbed in the main cavity is detected in vacuum and at ambient pressure. While the non-equivalence of SIAR in vacuum

Table 2. Radiant Power Measurement Results in Vacuum

	(1)	(2)	(3)	**Average**
$S_{VE} = S_{VR}$ (V/W)	70.201	70.042	69.975	70.073
P_1 (mW)	38.772	39.668	39.564	
P_2 (mW)	77.858	78.822	78.668	
V_{E1} (V)	5.457	5.513	5.500	
V_{E2} (V)	5.625	5.685	5.666	
Absorbed Radiant Power in Vacuum (mW)	36.699	36.704	36.733	36.712

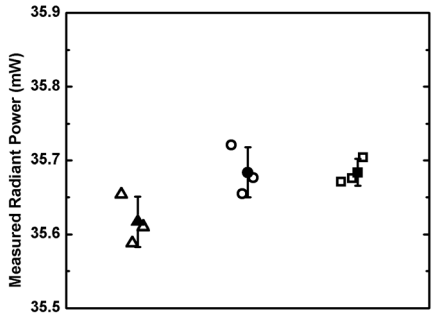

Fig. 4. Effect of non-equivalence correction of SIAR. Measured radiant power absorbed in the main cavity of SIAR with (○) and without (Δ) non-equivalence corrected at ambient pressure, and respective average value (corrected (•) and uncorrected (▼)) with error bar. The measured radiant power in vacuum (□) with atmospheric absorption corrected and the average value (■) with error bar are also shown.

is reasonably ignored, the radiative heating sensitivity at ambient pressure is acquired, which reveals a difference of the order of 0.08%–0.27% compared with the electrical heating sensitivity in the same working environment. The correction for non-equivalence of SIAR at ambient pressure is quantitatively evaluated, and the calculation equation of the absorbed radiant power in the main cavity is modified. A systematic deviation of the order of 0.19% of radiant power measurement at ambient pressure is eliminated with non-equivalence corrected, thus the systematic error of radiant power measurement of SIAR is compensated.

This work was supported by the National Natural Science Foundation of China under Grant No. 41227003.

References

1. K. E. Trenberth, J. T. Fasullo, and J. Kiehl, Bull. Am. Meteorol. Soc. **90,** 311 (2009).
2. Z. Tao, D. Liu, Z. Zhong, B. Shi, M. Nie, X. Ma, and J. Zhou, Chin. Opt. Lett. **10,** 050101 (2012).
3. X. Xiong, M. Li, L. Jiang, and S. Feng, Chin. Opt. Lett. **11,** 100101 (2013).
4. C. G. Abbot, L. B. Aldrich, and W. H. Hoover, Ann. Astrophys. Obs. Smithsonian Inst. **6,** 163 (1942).
5. C. Fröhlich, Space Sci. Rev. **125,** 53 (2006).
6. L. J. Gray, J. Beer, M. Geller, J. D. Haigh, M. Lockwood, K. Matthes, U. Cabasch, D. Fleitmann, G. Harrison, L. Hood, J. Luterbacher, G. A. Meehl, D. Shindell, B. van Geel, and W. White, Rev. Geophys. **48,** RG4001 (2010).
7. X. Z. Chen, W. Fang, Y. P. Wang, Z. L. Yang, and X. Q. Quan, Acta Phys. Sin. **62,** 164211 (2013).
8. F. Hengstberger, Metrologia **13,** 69 (1977).
9. R. W. Brusa and C. Fröhlich, Appl. Opt. **25,** 4173 (1986).
10. G. Kopp and G. Lawrence, Sol. Phys. **230,** 91 (2005).
11. G. Kopp and J. L. Lean, Geophys. Res. Lett. **38,** L01706 (2011).
12. M. Meftah, S. Dewitte, A. Irbah, A. Chevalier, C. Conscience, D. Crommelynck, E. Janssen, and S. Mekaoui, Sol. Phys. **289,** 1885 (2014).
13. C. Fröhlich, J. Romero, and H. Roth, Sol. Phys. **162,** 101 (1995).
14. W. Fang, B. Yu, H. Yao, Z. Li, C. Gong, and X. Jin, Acta Opt. Sin. **23,** 112 (2003).
15. W. Fang and B. X. Yu, Proc. SPIE **3501,** 469 (1998).
16. B. Yu, H. Yao, and W. Fang, Acta Opt. Sin. **25,** 786 (2005).